Purdue University
Purdue e-Pubs

Birck and NCN Publications | Birck Nanotechnology Center

6-1-2009

Thermal conductivity of bismuth telluride nanowire array-epoxy composite

Kalapi G. Biswas
Purdue University - Main Campus, kgbiswas@purdue.edu

Timothy D. Sands
Birck Nanotechnology Center, Purdue University, tsands@purdue.edu

Baratunde Cola
Purdue University - Main Campus

Xianfan Xu
Birck Nanotechnology Center, School of Materials Engineering, Purdue University, xxu@purdue.edu

Follow this and additional works at: http://docs.lib.purdue.edu/nanopub

Part of the Nanoscience and Nanotechnology Commons

Biswas, Kalapi G.; Sands, Timothy D.; Cola, Baratunde; and Xu, Xianfan, "Thermal conductivity of bismuth telluride nanowire array-epoxy composite" (2009). *Birck and NCN Publications.* Paper 393.
http://docs.lib.purdue.edu/nanopub/393

This document has been made available through Purdue e-Pubs, a service of the Purdue University Libraries. Please contact epubs@purdue.edu for additional information.

Thermal conductivity of bismuth telluride nanowire array-epoxy composite

Kalapi G. Biswas,[1,a)] Timothy D. Sands,[1] Baratunde A. Cola,[2] and Xianfan Xu[2]
[1]*School of Materials Engineering, Birck Nanotechnology Center, Purdue University, West Lafayette, Indiana 47907, USA*
[2]*School of Mechanical Engineering, Birck Nanotechnology Center, Purdue University, West Lafayette, Indiana 47907, USA*

(Received 12 April 2009; accepted 1 May 2009; published online 4 June 2009)

Electrodeposition of nanowire array in porous anodic alumina (PAA) templates combine the performance benefits offered by crystallographic texture control, lattice thermal conductivity suppression through boundary scattering of phonons, elastic relaxation of misfit strain, and scalablity essential for high efficiency thermoelectric devices. The template material, however, can serve as a thermal shunt thereby reducing the effective thermoelectric performance. Here, we demonstrate a process of minimizing the parasitic thermal conduction by replacing the PAA matrix with SU-8 ($\kappa \sim 0.2$ W/m K). We report a reduction in the performance penalty from 27% for Bi_2Te_3/PAA to ~5% for Bi_2Te_3/SU-8 nanocomposite by thermal conductivity measurements using a photoacoustic technique. © *2009 American Institute of Physics*. [DOI: 10.1063/1.3143221]

The thermal-to-electrical energy conversion efficiency of a thermoelectric material is given by its figure of merit, $ZT = \sigma \cdot S^2 T/\kappa$, where σ is the electrical conductivity in units of (Ω^{-1} m^{-1}), S is the Seebeck coefficient in units of (V/K), and κ is the thermal conductivity in units of (W/m K). Bulk materials based on Bi_2Te_3 and its alloys have been known as the best thermoelectric materials for applications near room temperature, delivering ZT values as high as 1. Recently, ball-milled, hot-pressed nanocrystalline bulk $(Bi,Sb)_2Te_3$ alloys have shown ZT values of ~1.4 in the temperature range of 340–370 K.[1,2] Epitaxial nanostructured thin films have exhibited enhanced ZT values, such as a reported ZT at 300 K of 2.4 for a Bi_2Te_3/Sb_2Te_3 superlattice grown by molecular beam epitaxy.[3] Bi_2Te_3-based materials, when grown in the form of nanowire arrays, may be expected to deliver even higher ZT values than their bulk and thin film counterparts due to enhanced phonon scattering, elastic relaxation of lattice misfit strain, texture control, and scalability to thicknesses required for thermoelectric applications.

The templated electrodeposition technique[4–9] employing porous anodic alumina (PAA) templates[10–14] has been widely used for the fabrication of high density, ordered nanowire arrays for thermoelectric applications. The nanowire/PAA composite provides an opportunity to engineer high density, high aspect ratio, ordered, and texture-controlled nanowire arrays in a PAA matrix, yielding a mechanically robust composite as is necessary to assemble the thermoelectric legs into an array of *p-n* couples. PAA, however, has a reported thermal conductivity of 1.7 W/m K,[15] which is comparable to that of the Bi_2Te_3 nanowire array,[5,16] thus the PAA matrix will act as a parasitic thermal shunt, reducing the effective ZT of the composite, ZT_{comp}. Based on a simple effective medium model that neglects the effects of solid-solid interfaces that are parallel to the temperature gradient, the ZT of the nanowire/matrix composite is given by $ZT_{comp} = ZT_{nw}\{1 + (\kappa_m/\kappa_{nw})[(1/f_{nw}) - 1]\}^{-1}$, where ZT_{nw} is the ZT value of the nanowire, κ_m is the thermal conductivity of the matrix, κ_{nw} is thermal conductivity of the nanowire, and f_{nw} is the volume filling fraction of the nanowires in the composite. To mitigate the detrimental effects of the matrix, the nanowire volume fraction should be maximized and the thermal conductivity of the matrix should be minimized.

If the lattice thermal conductivity of the nanowire can be reduced to values that are close to the theoretical minimum for Bi_2Te_3, ~0.25 W/m K,[5] a matrix with a thermal conductivity below 0.25 W/m K will be required to achieve a composite lattice thermal conductivity below 0.25 W/m K. Parylene-N, a vapor-deposited low thermal conductivity polymer (κ=0.125 W/m K) has been previously explored as a supporting matrix for embedded Si nanowire arrays with f_{nw}=0.02.[17] However, due to the high aspect ratio of the template channels, region between the nanowires (height:diameter ~800:1), and pore volume fraction ($f_{nw} \sim 0.7$) in PAA templates, parylene would tend to form a continuous film building up over the nanowire sidewalls and closing the channels.[18] In this work, we demonstrate a process flow to overcome the challenge of the parasitic thermal shunt in the nanowire array composites by fabricating dense, textured, nanowire arrays in a PAA matrix and then replacing the PAA matrix with epoxy resin.

The criteria for selection of epoxy resin for matrix infiltration included thermal conductivity, viscosity, wetting and adhesion, mechanical stability, shrinkage, and thermal stability. A commercially available epoxy resin, SU-8, which is widely used in the microelectronic industry for high-aspect-ratio and three-dimensional lithographic patterning, was chosen for infiltrating the nanowire array. SU-8 is also used as a permanent and functional material in silicon-on-insulator technologies.[19,20] The epoxy resin SU-8 has a thermal conductivity κ=0.2 W/m K,[21] which is an order of magnitude lower than that of the PAA matrix. Preliminary results describing the replacement of SU-8 with PAA were reported previously.[22] In the present work, we describe the fabrication process and demonstrate the efficacy of this approach with measurements of thermal conductivity.

Bi_2Te_3 nanowires were synthesized by galvanostatic electrodeposition into PAA templates (Anodisc 13, 200 nm diameter, Whatman Inc.). The templates were pore widened

[a)]Electronic mail: kgbiswas@purdue.edu.

 © 2009 American Institute of Physics

Downloaded 29 Jun 2009 to 128.46.220.88. Redistribution subject to AIP license or copyright; see http://apl.aip.org/apl/copyright.jsp

TABLE I. SU-8 processing steps and optimized baking time for nanowire array infiltration.

SU-8 2005 viscosity (cst)	Layer thickness (μm)	Soft bake at 65 °C (min)	Soft bake at 95 °C (min)	Post exposure bake at 65 °C (min)	Post exposure bake at 95 °C (min)	Hard bake at 150 °C (min)
45	40	2	30	1	10	30

using a 3 wt % KOH/ethylene glycol solution for achieving $72\% \pm 2.5\%$ porosity. Platinum was e-beam evaporated on one side of the template to serve as a back electrode for electrodeposition. The electrolyte solution consisted of $0.035M$ $Bi(NO_3)_3 \cdot 5\ H_2O$ (Alfa Aesar, 99.999%) and $0.05M$ $HTeO_2$ (Te, Alfa Aesar, 99.999%) in $1M$ nitric acid, and a pH=1 was maintained throughout the process. The nanowires were electrodeposited for a period of 2–3 h depending on the thickness desired, using 3 s pulses of current density 5 mA/cm^2 followed by a standby period of 3 s. Following synthesis, the nanowire arrays were mechanically planarized to overcome any overgrowth or nonuniformity in nanowire lengths.[23]

To fabricate nanowire array/SU-8 composites, the PAA template was entirely removed by etching in a 3 wt % KOH solution for 24 h. To prevent collapse of freestanding Bi_2Te_3 nanowires as a consequence of capillary forces acting on nanowire sidewalls, the rinsing procedure with de-ioinized water (72 $mN\ m^{-1}$) was followed by a lower surface tension solvent, isopropanol (21.8 $mN\ m^{-1}$). The isopropanol was allowed to evaporate in the solvent hood. This procedure yielded 40 μm thick freestanding planarized Bi_2Te_3 nanowire arrays. SU-8 2005 was spin coated on the nanowire array at 2000 rpm for 30 s to obtain a resin matrix thickness of 40 μm. The assembly was then dipped in isopropanol for 1 s to remove excess SU-8 on the top surface. This was followed by a 30 min UV processing in a UV flood curing system (Cure Zone 2, 400 W Hg lamp, intensity 30 $mW\ cm^{-2}$). SU-8 resin contains acid-labile groups and a photoacid generator, which on irradiation decompose to generate a low concentration of catalyst acid. Subsequent heating of the polymer activates crosslinking and regenerates the acid catalyst. Solvent removal by soft baking is a crucial step contributing to overall film internal stress during processing through volume shrinkage and mechanical stress accumulation.[24] Optimizing this step improves the resist-nanowire sidewall adhesion. Irradiation followed by postexposure bake leads to an increased degree of crosslinking and stabilization. Since the purpose of the SU-8 matrix is to provide a permanent structural framework for the thermoelectric element, the composite must be hard baked, typically at 150 °C. The SU-8 processing steps and baking time are presented in Table I. To accommodate the large SU-8 thickness (40 μm), all baking steps were carried out on a leveled hotplate (by conduction) to avoid dried layer formation on the surface, hindering diffusion of solvent from the interior.

Figures 1 and 2 compare field emission scanning electron microscopy (FESEM) cross-sectional images of the nanowire array/PAA composite and nanowire array/SU-8 composite. The image of the nanowire/SU-8 composite reveals that the nanowires are completely embedded in the polymer matrix with crystallographic cleavage planes evident in the Bi_2Te_3. A higher magnification image of the composite cross section clearly shows that the fracture proceeded by crack propagation through the nanowire, and not through the interface of the nanowire and SU-8 matrix, suggesting that the nanowire /SU-8 interface is of high structural integrity. On the other hand, the FESEM image obtained from the nanowire array/PAA composite shows that the fracture propagates preferentially along the interface between the nanowire and PAA. The crystallographic cleavage planes observed in the fractured nanowire array/SU-8 composites can be attributed to the weak van der Waals bonding between the Te–Te atomic planes in Bi_2Te_3 crystal structure,[25,26] which is preferentially oriented in the nanowire arrays such that the c-axis of the pseudohexagonal unit cell is perpendicular to the nanowire axis.

A photoacoustic (PA) technique was used to measure the thermal conductivity of the nanowire array composites. A modulated laser was used to heat the surface of the sample, which was surrounded by a sealed acoustic chamber filled with He gas. The sample and a quartz reference were coated with a thin metal film (Ti with a thickness of approximately 80 nm) to absorb the laser energy. The laser was a continuous power fiber laser (1064 nm) and an acoustic-optical chopper was used to modulate the beam in the 1–10 kHz range. A microphone mounted in the side wall of the acoustic chamber was used to measure the amplitude and phase shift of the pressure signal. The measured acoustic response was related to thermal properties of the sample using a one-dimensional heat conduction model.[27] Details of the PA measurement technique are provided elsewhere.[27–29]

The 300 K thermal conductivity values obtained by the PA technique were 1.4 ± 0.07 W/m K for the Bi_2Te_3 nanowire array/PAA composite and 1.1 ± 0.06 W/m K for Bi_2Te_3 nanowire array/SU-8 composite. The thermal conductivity of the PAA matrix alone (i.e., PAA/air composite) was measured as 0.38 ± 0.02 W/m K. Assuming that the volume fraction of the nanowire material is f_{nw}, and that the composite is dense such that the volume fraction of the matrix is $1-f_{nw}$, the thermal conductivity of the Bi_2Te_3 nanowire array composite can be estimated as $f_{nw}\,\kappa_{nw}+(1-f_{nw})\kappa_m$, where κ_{nw} and κ_m are the thermal conductivities of the nanowire and the matrix, respectively. Taking into account that the porosity fraction in the PAA template was

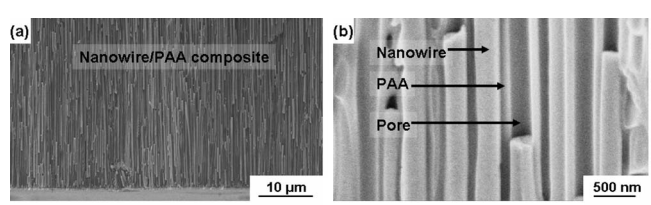

FIG. 1. (a) FESEM image showing the pristine fractured cross section of an as-grown Bi_2Te_3 nanowire array/PAA composite. (b) A magnified view of the composite cross section that shows that the crack through the interface between the PAA and the nanowire rather than through the nanowire, in contrast to the observed behavior of cracks in the nanowire/SU-8 composite [Figs. 2(a) and 2(b)].

Downloaded 29 Jun 2009 to 128.46.220.88. Redistribution subject to AIP license or copyright; see http://apl.aip.org/apl/copyright.jsp

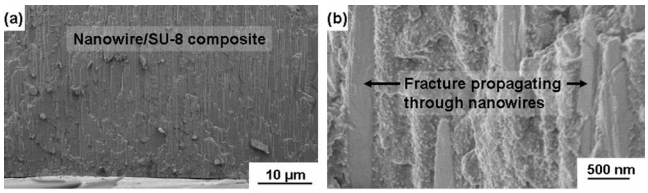

FIG. 2. (a) FESEM image showing the pristine fractured cross section of a Bi_2Te_3 nanowire array/SU-8 composite. The nanowires are embedded in the SU-8 epoxy matrix confirming complete infiltration of the epoxy. (b) A magnified view of the composite cross-section that shows that the fracture plane propagates through the nanowire—exposing crystallographic cleavage planes in Bi_2Te_3—and not through the interface between the nanowire and the SU-8 epoxy.

0.72 ± 0.025, the effective PAA thermal conductivity is 1.31 ± 0.1 W/m K. This value can be used to estimate the contribution from the Bi_2Te_3 nanowires in the composite, which is calculated to be 1.44 ± 0.1 W/m K. In the second case, the thermal conductivity of the Bi_2Te_3 nanowire array/SU-8 composite was measured to be 1.1 ± 0.06 W/m K. Using the volume fraction and thermal conductivity of SU-8 as 0.28 ± 0.025 and 0.2 W/m K, respectively, the effective thermal conductivity of the Bi_2Te_3 nanowires in the composite is 1.45 ± 0.09 W/m K. The thermal conductivity values obtained for Bi_2Te_3 nanowires lie within the range of experimental error and in conformation with previously reported data.[5]

In conclusion, we have demonstrated a method for overcoming a significant obstacle to utilizing nanowire arrays as thermoelectric materials. The dense (72% nanowire volume fraction) and mechanically robust nanowire array/SU-8 composites fabricated by replacing the PAA template substantially reduce the matrix thermal shunt. Thermal conductivity measurements by the PA technique reflect a 21% reduction in the composite's thermal conductivity when the PAA matrix (κ=1.31 W/m K) is replaced with SU-8 epoxy resin (κ =0.2 W/m K). This study with relatively large diameter, nonalloyed Bi_2Te_3 nanowires represents a baseline for the improvements that might be expected from replacing PAA with SU-8. For example, replacement of PAA with SU-8 in a composite with f_{nw}=0.7 and smaller diameter alloyed nanowires with an effective thermal conductivity of 1 W/m K would reduce the composite thermal conductivity from 1.09 to 0.76 W/m K, thereby increasing the *ZT* of the composite by 44%.

This work was supported by a grant from the Office of Naval Research (Grant No. N000140610641).

[1]Y. Ma, Q. Hao, B. Poudel, Y. Lan, B. Yu, D. Wang, G. Chen, and Z. Ren, Nano Lett. **8**, 2580 (2008).
[2]B. Poudel, Q. Hao, Y. Ma, Y. C. Lan, A. Minnich, B. Yu, X. Yan, D. Z. Wang, A. V. Muto, D. Vashaee, X. Y. Chen, J. M. Liu, M. S. Dresselhaus, G. Chen, and Z. F. Ren, Science **320**, 634 (2008).
[3]R. Venkatasubramanian, E. Siivola, T. Colpitts, and B. O'Quinn, Nature (London) **413**, 597 (2001).
[4]S. A. Sapp, B. B. Lakshmi, and C. R. Martin, Adv. Mater. (Weinheim, Ger.) **11**, 402 (1999).
[5]D.-A. Borca-Tasciuc, G. Chen, A. Prieto, M. S. Martín-González, A. Stacy, T. Sands, M. A. Ryan, and J. P. Fleurial, Appl. Phys. Lett. **85**, 6001 (2004).
[6]C. G. Jin, X. Q. Xiang, C. Jia, W. F. Liu, W. L. Cai, L. Z. Yao, and X. G. Li, J. Phys. Chem. B **108**, 1844 (2004).
[7]M. S. Sander, A. L. Prieto, R. Gronsky, T. Sands, and A. M. Stacy, Adv. Mater. (Weinheim, Ger.) **14**, 665 (2002).
[8]M. S. Sander, R. Gronsky, T. Sands, and A. M. Stacy, Chem. Mater. **15**, 335 (2003).
[9]W. Wang, Q. Huang, F. Jia, and J. Zhu, J. Appl. Phys. **96**, 615 (2004).
[10]H. Masuda, H. Yamada, M. Satoh, H. Asoh, M. Nakao, and T. Tamamura, Appl. Phys. Lett. **71**, 2770 (1997).
[11]O. Jessensky, F. Muller, and U. Gosele, Appl. Phys. Lett. **72**, 1173 (1998).
[12]W. Lee, R. Ji, U. Gosele, and K. Nielsch, Nature Mater. **5**, 741 (2006).
[13]H. Masuda, K. Yada, and A. Osaka, Jpn. J. Appl. Phys., Part 2 **37**, L1340 (1998).
[14]K. Nielsch, Nano Lett. **2**, 677 (2002).
[15]D. A. Borca-Tasciuc and G. Chen, J. Appl. Phys. **97**, 084303 (2005).
[16]J. H. Zhou, C. G. Jin, J. H. Seol, X. G. Li, and L. Shi, Appl. Phys. Lett. **87**, 133109 (2005).
[17]A. R. Abramson, W. C. Kim, S. T. Huxtable, H. Yan, Y. Wu, A. Majumdar, C.-L. Tien, and P. Yang, J. Microelectromech. Syst. **13**, 505 (2004).
[18]J. R. Lim, J. F. Whitacre, J. P. Fleurial, C. K. Huang, M. A. Ryan, and N. V. Myung, Adv. Mater. (Weinheim, Ger.) **17**, 1488 (2005).
[19]A. D. Campo and C. Greiner, J. Micromech. Microeng. **17**, R81 (2007).
[20]E. H. Conradie and D. F. Moore, J. Micromech. Microeng. **12**, 368 (2002).
[21]MicroChem (http://www.microchem.com/resources/app_notes.htm).
[22]K. Biswas, V. Rawat, M. DaSilva, and T. Sands, 2nd Energy Nanotechnology International Conference, ASME, 2007 (unpublished), p. 45029.
[23]K. Biswas, Y. Qin, M. DaSilva, R. Reifenberger, and T. Sands, Phys. Status Solidi A **204**, 3152 (2007).
[24]R. L. Barber, M. K. Ghantasala, R. Divan, K. D. Vora, E. C. Harvey, and D. C. Mancini, Microsyst. Technol. **11**, 303 (2005).
[25]G. E. Shoemake, J. A. Rayne, and J. R. W. Ure, Phys. Rev. **185**, 1046 (1969).
[26]M. H. Francombe, Br. J. Appl. Phys. **9**, 415 (1958).
[27]H. Hu, X. Wang, and X. C. Xu, J. Appl. Phys. **86**, 3953 (1999).
[28]X. Wang, H. Hu, and X. Xu, ASME J. Heat Transfer **123**, 138 (2001).
[29]B. A. Cola, R. Karru, C. Cheng, X. Xu, and T. S. Fisher, IEEE Trans. Compon. Packag. Technol. **31**, 46 (2008).

Downloaded 29 Jun 2009 to 128.46.220.88. Redistribution subject to AIP license or copyright; see http://apl.aip.org/apl/copyright.jsp